Tyrosine phosphorylation of the AMPA receptor subunit GluA2 gates homeostatic synaptic plasticity

Adeline J. H. Yong[a,b], Han L. Tan[a,b], Qianwen Zhu[a,b], Alexei M. Bygrave[a,b], Richard C. Johnson[a,b], and Richard L. Huganir[a,b,1]

[a]Department of Neuroscience, Johns Hopkins University School of Medicine, Baltimore, MD 21205; and [b]Kavli Neuroscience Discovery Institute, Johns Hopkins University, Baltimore, MD 21205

Contributed by Richard L. Huganir, January 14, 2020 (sent for review October 22, 2019; reviewed by Hee Jung Chung and Stephen J. Moss)

Hebbian plasticity, comprised of long-term potentiation (LTP) and depression (LTD), allows neurons to encode and respond to specific stimuli; while homeostatic synaptic scaling is a counterbalancing mechanism that enables the maintenance of stable neural circuits. Both types of synaptic plasticity involve the control of postsynaptic α-amino-3-hydroxy-5-methyl-4-isoxazolepropionic acid (AMPA) receptor (AMPAR) abundance, which is modulated by AMPAR phosphorylation. To address the necessity of GluA2 phospho-Y876 in synaptic plasticity, we generated phospho-deficient GluA2 Y876F knock-in mice. We show that, while GluA2 phospho-Y876 is not necessary for Hebbian plasticity, it is essential for both in vivo and in vitro homeostatic upscaling. Bidirectional changes in GluA2 phospho-Y876 were observed during homeostatic scaling, with a decrease during downscaling and an increase during upscaling. GluA2 phospho-Y876 is necessary for synaptic accumulation of glutamate receptor interacting protein 1 (GRIP1), a crucial scaffold protein that delivers AMPARs to synapses, during upscaling. Furthermore, increased phosphorylation at GluA2 Y876 increases GluA2 binding to GRIP1. These results demonstrate that AMPAR trafficking during homeostatic upscaling can be gated by a single phosphorylation site on the GluA2 subunit.

AMPAR | GluA2 | GluA2 tyrosine phosphorylation | homeostatic plasticity | GRIP1

The ability of neurons to alter the strength of their synaptic inputs bidirectionally in response to different stimuli is known as synaptic plasticity. Hebbian plasticity is the most well understood and consists of long-term potentiation (LTP) and long-term depression (LTD). This process occurs in an input-specific manner, wherein the strength of stimulated synapses changes relative to nearby unstimulated synapses (1). Synaptic plasticity allows the brain to encode and respond to different stimuli; learning and memory, for example, is widely believed to involve Hebbian plasticity.

In the midst of changes in synaptic strength and number, homeostatic plasticity is a counterbalancing mechanism that allows neural circuits to maintain stable activity. One type of homeostatic plasticity is synaptic scaling, where neurons respond to a sustained destabilization in network activity by adjusting their activity toward a set point while preserving the relative synaptic weight differences among them. This helps to offset the destabilizing effects of continued LTP or LTD and maintain network stability (2–4). At excitatory synapses, chronic activity blockade induces upscaling whereby neurons increase their synaptic strength, while persistent hyperactivity results in downscaling, whereby neurons decrease their synaptic strength.

The dynamic control of α-amino-3-hydroxy-5-methyl-4-isoxazolepropionic acid receptor (AMPAR) expression at the synaptic surface is a crucial mechanism for both Hebbian plasticity and synaptic scaling (5). Tetrameric AMPARs are the major excitatory postsynaptic receptors composed of subunits GluA1 through GluA4. Many proteins form scaffolding complexes that bind to the AMPAR cytoplasmic tail to differentially traffic and/or sequester them in distinct cellular compartments (6). Posttranslational modifications, particularly AMPAR phosphorylation(s) on the cytoplasmic C-terminal tails, are known to modulate binding of these proteins to AMPARs and affect AMPAR trafficking (5).

GluA1 phosphorylation has been studied extensively in Hebbian plasticity. LTP is facilitated by increases in phosphorylation of GluA1 S845 and GluA1 S831, while dephosphorylation of GluA1 S845 is associated with LTD (5). Synaptic scaling also involves GluA1 phosphorylation. Changes in the phosphorylation of GluA1 S845, but not GluA1 S831, are necessary for both tetrodotoxin (TTX) -induced and visual-deprivation–induced upscaling (7, 8). Within GluA2, S880 is a well-characterized phosphorylation site that is critical for cerebellar LTD (9). During cerebellar LTD, protein kinase C phosphorylates GluA2 S880, which disrupts glutamate receptor interacting protein 1 (GRIP1) binding, thereby promoting GluA2 binding with protein interacting with C-kinase 1 (PICK1) and AMPAR endocytosis (10, 11). Additionally, much interest has been generated over the three tyrosine sites (Y869, Y873, Y876; 3Y) on the GluA2 C terminus that have been suggested to be phosphorylated (12, 13). Multiple groups report that infusion of the GluA2 3Y peptide (YKEGYNVYG) in slices, as well as in animals, can block various forms of LTD including mGluR-LTD (14) and *N*-methyl-D-aspartate receptor (NMDAR)-LTD (15–17), while LTP appears normal (18). Outside the hippocampus, the 3Y peptide also blocks LTD in the nucleus accumbens (18) and lateral amygdala (19, 20). Furthermore,

Significance

Throughout an organism's life span, neural circuits mediate sensory and cognitive processing via synaptic plasticity, which involves synapse-specific Hebbian plasticity and network-level homeostatic plasticity. Synaptic strengthening and weakening are finely tuned by changes in postsynaptic α-amino-3-hydroxy-5-methyl-4-isoxazolepropionic acid (AMPA) -type glutamate receptors (AMPARs). We have elucidated a biochemical regulation of AMPARs that is specific to homeostatic synaptic plasticity while sparing Hebbian plasticity mechanisms. Specifically, phosphorylation of the AMPAR subunit, GluA2, at tyrosine-876 is required for homeostatic synaptic strengthening by dictating GluA2 binding to glutamate receptor interacting protein 1 (GRIP1), a scaffolding protein crucial for synaptic upscaling. This finding elucidates a mechanism through which neurons can maintain a range of synaptic signaling while not compromising their responsiveness to subsequent synaptic activity.

Author contributions: A.J.H.Y. and R.L.H. designed research; A.J.H.Y., H.L.T., Q.Z., and A.M.B. performed research; R.C.J. contributed new reagents/analytic tools; A.J.H.Y. and Q.Z. analyzed data; and A.J.H.Y. and R.L.H. wrote the paper.

Reviewers: H.J.C., University of Illinois at Urbana–Champaign; and S.J.M., Tufts University.

The authors declare no competing interest.

[1]To whom correspondence may be addressed. Email: rhuganir@jhmi.edu.

This article contains supporting information online at https://www.pnas.org/lookup/suppl/doi:10.1073/pnas.1918436117/-/DCSupplemental.

First published February 18, 2020.

mGluR-LTD is associated with tyrosine dephosphorylation of GluA2 (21, 22) and is blocked by inhibitors of tyrosine phosphatases (21). Of the three tyrosine sites, only Y876 has been validated to be phosphorylated by Src-family protein tyrosine kinases, including Fyn and Src (13, 14, 23). A recent study described dephosphorylation of Y876 during mGluR-LTD, causing BRAG2 binding to GluA2, ADP-ribosylation factor 6 (Arf-6) activation, and AMPAR internalization (14). While these studies in concert lend strong support that GluA2 tyrosine phosphorylation, particularly Y876 phosphorylation, is associated with LTD, what remains unaddressed is the necessity of GluA2 tyrosine phosphorylation for LTD. Additionally, GluA2 tyrosine phosphorylation has been implicated in synaptic scaling. Phosphorylation of GluA2 3Y increases during TTX-induced upscaling and decreases during bicuculline-induced downscaling (24). However, the exact tyrosine residue(s) and whether these changes are necessary for AMPAR trafficking during homeostatic scaling remain elusive.

In this study, we made a phosphodeficient knock-in mouse, GluA2 Y876F, to address the necessity of GluA2 Y876 in Hebbian plasticity and synaptic scaling. Surprisingly, we found that Hebbian plasticity appeared normal while upscaling induced in vitro with TTX or in vivo with visual deprivation was deficient in GluA2 Y876F mice. We observed that upscaling increased in GluA2 Y876 phosphorylation while downscaling led to a decrease. Moreover, the postsynaptic GRIP1 increase observed during upscaling in wild-type (WT) mice was abolished in GluA2 Y876F mutant mice. Finally, we show that increasing GluA2 Y876 phosphorylation can increase GRIP1 binding. Thus, we demonstrate the necessity of phospho-Y876 and the underlying mechanisms for its importance in synaptic upscaling.

Results

Characterization of Y876F Knock-In Mice and Discovery of GluA3 Phospho-Y881. We generated GluA2 Y876F knock-in mice that are phosphodeficient at Y876 by homologous recombination (Y876F; *SI Appendix*, Fig. S1*A*) and verified them with Southern blotting (*SI Appendix*, Fig. S1*B*) and PCR (*SI Appendix*, Fig. S1*C*). Western blots were performed to confirm that GluA2 Y876 is not phosphorylated in these mice. Cultured cortical neurons obtained from Y876F and WT mice were treated either with the tyrosine phosphatase inhibitor sodium orthovanadate (NV) or with a Src tyrosine kinase inhibitor, 4-amino-5-(4-chlorophenyl)-7-(dimethylethyl)pyrazolo[3,4-d]pyrimidine (PP2), and compared with untreated controls. In WT neurons, we observed an increase in the phospho-Y876 (pY876) signal with NV and a decrease with PP2 (Fig. 1*A*). Unexpectedly, this signal was present, albeit diminished, in Y876F neurons (Fig. 1*A*). To address this, we verified the specificity of the pY876 antibody using overexpression of WT or Y876F GluA2, together with Fyn or v-Src (kinases that phosphorylate GluA2 Y876) in human embryonic kidney 293 (HEK293) cells (*SI Appendix*, Fig. S3*C*). A clear signal was present with overexpression of WT GluA2 with Fyn or v-Src but not with Y876F GluA2 (*SI Appendix*, Fig. S3*C*). Lambda phosphatase treatment of the Western blot membrane also confirmed the phospho-specificity of the signal (*SI Appendix*, Fig. S3*C*). Therefore, we deduced that the residual pY876 signal observed in Y876F cultures was not due to nonspecificity of the antibody. Since GluA3 has a similar C terminus (*SI Appendix*, Fig. S3*B*), we hypothesized that GluA3 might be phosphorylated on an analogous tyrosine residue (Y881), and that our antibody was recognizing this site. Using a full denaturing lysis condition, we separately immunoprecipitated the GluA2 and GluA3 subunits and observed that GluA2 phospho-Y876 was no longer detected in the Y876F knock-in mice (Fig. 1*B*). Interestingly, in both WT and Y876F knock-in mice, the pY876 antibody detected a signal from the GluA3 subunit, which increased with NV and decreased with PP2 (Fig. 1*C*). To confirm this finding, we repeated this with HEK293 cell transfection experiments, similar to the one discussed above but with GluA3, and validated that the pY876 antibody also recognizes phospho-Y881 (pY881) of GluA3 (*SI Appendix*, Fig. S3*D*). Thus, in addition to confirming that Y876F mice are phospho-deficient at GluA2 Y876, we discovered a phosphorylation of GluA3 at Y881 by Src-family tyrosine kinases. Using our GluA2 pS880 antibody, we also found that GluA3 S885, an analogous site on GluA3, can be phosphorylated. We verified that our pS880 antibody is phospho-specific for both GluA2 pS880 and GluA3 pS885 (*SI Appendix*, Fig. S4), which might explain the residual signal from K882A knock-in mice (*SI Appendix*, Fig. S4 *E* and *F*) observed by Steinberg et al. (9).

Since both GluA2 and GluA3 can be phosphorylated at Y876 or Y881, we wanted to test the possibility that the lack of GluA2 Y876 phosphorylation in Y876F knock-in mice might be compensated for by an increase in GluA3 Y881 phosphorylation. We treated neurons with NV or PP2, or used untreated controls, and performed a full denaturing lysis followed by immunoprecipitation for GluA3 (Fig. 1*C*). Basal levels of GluA3 phospho-Y881 and its regulation by NV or PP2 were found to be unchanged in Y876F mice (Fig. 1*D*).

GluA2 Y876F Knock-In Mice Have Reduced Basal Synaptic GluA2. To study whether GluA2 Y876F mice have altered total or synaptic protein expression, we performed subcellular fractionation preparations from hippocampal tissue obtained from 3- to 6-mo-old Y876F mice and their WT littermates (Fig. 1*E*). Western blots were conducted from the postnuclear supernatant 1 (S1) fraction as a proxy of total protein and from the postsynaptic density (PSD) pellet, which is enriched for postsynaptic proteins (Fig. 1*F*). Total expression was unchanged for AMPARs (GluA1-3), AMPAR-scaffolding proteins such as GRIP1, GRIP2, and PICK1, other glutamate receptors like mGluR1, mGluR5, and GluN1, and trafficking proteins such as Sec 8 and Syntaxin 13 (Fig. 1*G* and *SI Appendix*, Fig. S1*D*). However, within the PSD there was a significant decrease in GluA2, indicating that phospho-Y876 is important for maintaining GluA2 at the synapse under basal conditions (Fig. 1*H*).

There were no changes in total or synaptic phosphorylation of S880/885 (Fig. 1 *G* and *H*), a site close to Y876/881 that is known to regulate GRIP1 binding. We also found that the affinities of the pY876 and pS880 antibodies are not affected by the phosphorylation status of the other site (*SI Appendix*, Fig. S5 *A–E*). Furthermore, we treated cortical cultures with NV and/or phorbol 12-myristate 13-actetate (PMA), a protein kinase C (PKC) activator, and found that phosphorylation of Y876 or S880 can be regulated independently (*SI Appendix*, Fig. S5). The remaining pY881 signal in Y876F mice is about 30% of the pY876/881 signal from WT mice, in both S1 and PSD fractions (Fig. 1 *G* and *H*), indicating that GluA2 phosho-Y876 contributes to ∼70% of the pY876/881 signal in WT mice. We also observed that synaptic GluN2A showed a small decrease, with no changes in total expression (*SI Appendix*, Fig. S1 *E* and *F*).

Additionally, we measured the number of excitatory synapses in cortical cultures by quantifying the number of GluA1 puncta and found no differences between WT and Y876F cultures (*SI Appendix*, Fig. S2), indicating that lack of GluA2 pY876 does not affect the number of excitatory synapses.

GluA2 Y876F Knock-In Mice Have Normal Hebbian Plasticity. Multiple studies utilizing the GluA2 3Y peptide containing the triple-tyrosine motif (Y869, Y873, and Y876) demonstrated that this peptide is able to block various forms of activity-dependent LTD in the hippocampus (12, 14, 17). While mGluR-LTD has been associated with GluA2 tyrosine dephosphorylation (21, 22, 25), one study narrowed this change to the Y876 site (14). In that study, dephosphorylation of phospho-Y876 was found to allow

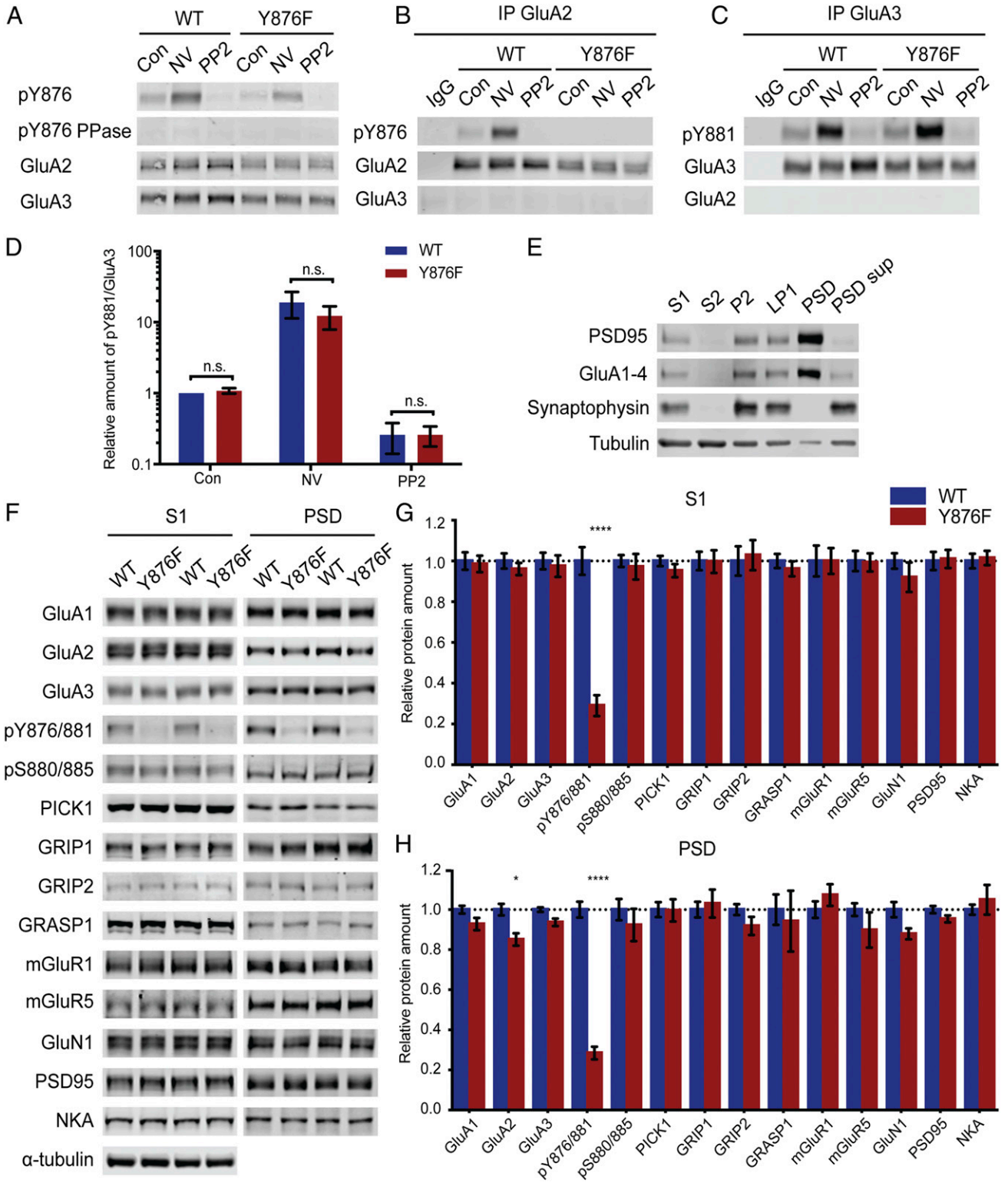

Fig. 1. Characterization of GluA2 Y876F knock-in mice. (*A–C*) Eighteen days in vitro (DIV18) cortical culture neurons from WT and Y876F knock-in mice were untreated (Con), treated with 1 μM NV overnight, or treated with 20 μM PP2 for 1 h followed by a fully denaturing lysis and Western blot (*A*) or IP for GluA2 (*B*) and GluA3 (*C*) and Western blot analysis. (*D*) Quantification of results from (*C*); values were normalized first to GluA3 and then to WT control. $n = 3$, two-way ANOVA. (*E* and *F*) Postsynaptic density preparation was conducted using hippocampi of 3 to 6-mo-old WT littermates and Y876F mice. (*E*) S1 (post-nuclear), S2 (cytosol), P2 (membrane), LP1 (synaptosome), PSD, and PSD supernatant fraction were collected for Western blot. (*F*) S1 (as a proxy for total protein) and PSD fractions were used for immunoblot. Representative immunoblots are shown. (*G*) Quantification of total proteins normalized to α-tubulin and WT controls from (*F*). $n = 12$, unpaired *t* test with Holmes-Sidak correction for multiple comparisons. (*H*) Quantification of synaptic proteins normalized to WT controls. $n = 11–12$, unpaired *t* test with Holmes-Sidak correction for multiple comparisons. $^{*}P < 0.05$, $^{*****}P < 0.0001$.

BRAG2 binding, resulting in AMPAR internalization during mGluR-LTD. Since the Y876F mice lack phospho-Y876, we hypothesized that, if dephosphorylation of Y876 is necessary, mGluR-LTD may be impaired in these mice. To address this, we performed field recordings at Schaffer collateral cornu ammonis (CA)1 synapses using acute hippocampal slices from 2- to 5-mo-old animals. After stable baseline recordings for 30 min, we used paired-pulse low-frequency stimulation (ppLFS) in the presence of 2-amino-5-phosphonopentanoic acid (APV) to induce mGluR-LTD (Fig. 2*A*). We observed that the resulting changes in field excitatory postsynaptic potentials (fEPSPs) were comparable between Y876F mice and WT littermates after mGluR-LTD (Fig. 2*B*), indicating that phospho-Y876 is not necessary for mGluR-LTD.

Several studies have shown that NMDAR-LTD can also be blocked by the GluA2 3Y peptide (15–17). Hence, low-frequency stimulation (LFS) was used to induce NMDAR-LTD (Fig. 2*C*). We found that NMDAR-LTD was equivalent between WT and Y876F littermates (Fig. 2*D*). Additionally, we noted that Y876F mice had normal NMDAR-LTP after theta-burst stimulation (TBS; Fig. 2 *E* and *F*). Thus, while phospho-Y876 regulates synaptic GluA2 at basal levels (Fig. 1*G*), Hebbian plasticity in the hippocampus appears largely intact in the Y876F knock-in mice.

In addition, we did not observe any significant differences in paired-pulse ratios (PPRs) between WT and Y876F mice (Fig. 2*H*), indicating that presynaptic function is largely normal in Y876F mice. Upon examination of input/output (I/O) relationships, we also found that synaptic strength was comparable between Y876F and WT mice under baseline conditions (Fig. 2*G*).

GluA2 Phospho-Y876 Is Required for In Vitro Upscaling. A previous study reported bidirectional changes in phosphorylation of GluA2 tyrosine residues during homeostatic synaptic scaling, using an antibody against three phospho-tyrosine residues on GluA2: 869, 873, and 876 (24). However, whether these change(s) are necessary for synaptic scaling is unclear. We tested the necessity of GluA2 pY876 in synaptic scaling using our phospho-deficient Y876F knock-in mice. WT and Y876F cultured mouse cortical neurons were treated for 48 h with TTX (a voltage-gated sodium channel antagonist) to decrease network activity or with bicuculline (Bic; a γ-aminobutyric acid [GABA] receptor antagonist) to increase network activity, well-established protocols that induce upscaling or downscaling, respectively (2, 4). Next, we conducted surface biotinylation, pull-down with neutravidin beads, and Western blot to measure levels of surface and total proteins. Consistent with previous studies, surface GluA1, GluA2, and GluA3 expression in WT neurons decreased in response to Bic, while surface GluA1 and GluA2 increased with TTX treatment (Fig. 3 *A* and *B*). In Y876F neurons, Bic reduced surface GluA1, GluA2, and GluA3 to an extent similar to that of WT neurons (Fig. 3 *A* and *B*). However, upscaling appeared to be deficient in Y876F cultured neurons, as TTX did not induce increases in surface GluA1 and GluA2 expression (Fig. 3 *A* and *B*). Meanwhile, the changes in total AMPAR expression for Bic and TTX treatment agreed with previous findings (7) and were comparable between WT and Y876F (Fig. 3*C*).

To validate these findings, we conducted surface staining of cultured cortical neurons. Bic treatment caused a decrease in surface GluA1 (Fig. 3 *D* and *F*) and GluA2 (Fig. 3 *E* and *G*) in both WT and Y876F neurons. In contrast, GluA1 and GluA2 scaled-up with TTX in WT neurons but not in Y876F neurons (Fig. 3 *D*–*G*). Furthermore, we recorded miniature excitatory postsynaptic currents (mEPSCs) from WT or Y876F neurons that were untreated or TTX-treated (Fig. 3*H*). We observed an increase in mEPSC amplitude in response to TTX in WT neurons but not in Y876F neurons (Fig. 3*I*), with no changes in mEPSC frequency (Fig. 3*I*), indicating that TTX treatment increased synaptic AMPAR expression in WT neurons but not in Y876F neurons. All together, these results demonstrate that GluA2 phospho-Y876 is required for TTX-induced upscaling.

GluA2 Phospho-Y876 Is Necessary for In Vivo Upscaling. Having identified that phosphorylation of Y876 is important for in vitro upscaling, we examined whether GluA2 Y876 phosphorylation is also necessary for upscaling in vivo. In the rodent, 2 or 7 d of binocular visual deprivation leads to an increase in excitatory synaptic transmission in the primary visual cortex (V1), which utilizes mechanisms similar to upscaling in vitro (26–29). Therefore, we visually deprived WT and Y876F mice by binocular enucleation, dissected V1 from these mice after 2 or 7 d, and performed subcellular fractionation to obtain the PSD fraction. We determined the levels of GluA1, GluA2, and GluA3 in WT and Y876F V1 PSD by Western blot (Fig. 4). Consistent with previous findings (26–29), there was an increase in AMPARs in PSD fractions after visual deprivation in WT mice, which showed increases in both GluA1 and GluA2 after enucleation (Fig. 4 *B* and *C*), with no changes in GluA3 (Fig. 4*D*). In contrast, this in vivo upscaling was not present in V1 PSD of Y876F mice (Fig. 4 *B* and *C*).

Synaptic Scaling Bidirectionally Regulates GluA2 Phospho-Y876 but Not GluA3 Phospho-Y881. Given that GluA2 phospho-Y876 is necessary for both in vitro and in vivo upscaling (Figs. 3 and 4), we wanted to investigate the regulation of phospho-Y876 during synaptic scaling. We treated rat cortical cultures for 48 h with TTX or Bic. We found that TTX treatment enhanced the phosphorylation of Y876/881 while Bic treatment decreased levels of phospho-Y876/881 (Fig. 5 *A* and *B*). To examine whether both GluA2 pY876 and GluA3 pY881 are regulated during synaptic scaling, we separately performed immunoprecipitations for GluA2 and GluA3 in completely denatured lysates (Fig. 5*C*), and discovered that phosphorylation of GluA2 Y876—but not GluA3 Y881—is bidirectionally regulated during synaptic scaling (Fig. 5*D*).

In contrast, a nearby phosphorylation site(s) on the C terminus of GluA2/3, S880/885, does not appear to be bidirectionally regulated during synaptic scaling. We observed a decrease in phospho-S880/885 with Bic but no changes with TTX (Fig. 5 *E* and *F*).

Furthermore, we studied GluA2 phospho-Y876 after visual-deprivation–induced upscaling. WT mice showed an increase in phospho-Y876/881 after enucleation (Fig. 5 *G* and *H*). However, no changes were found in GluA3 phospho-Y881 in Y876F mice (Fig. 5 *I* and *J*), indicating that the enhanced phosphorylation in WT mice came from an increase in GluA2 phospho-Y876.

GluA2 Phospho-Y876 Is Required for Increase in GRIP1 during Upscaling. GluA2 contains a postsynaptic density 95/discs large/zona occludens (PDZ) ligand, consisting of the amino acid sequence serine, valine, lysine, and isoleucine (SVKI), on its cytoplasmic tail that binds to the PDZ domains of GRIP1 and PICK1 (30). Both GRIP1 and PICK1 are important for regulating GluA2 localization (30). In particular, GRIP1 is crucial for activity-dependent trafficking of GluA2 and helps deliver AMPARs to synapses (31). GRIP1 is also necessary for upscaling, as either knock-out (32) or knock-down (33) of GRIP1 abolishes upscaling. During TTX-induced upscaling, more GRIP1 binds to GluA2 to facilitate trafficking and/or retention of AMPARs to synapses (32, 33). Surface biotinylation approaches are not able to measure changes in membrane-associated GRIP1 because it is an intracellular protein. Hence, we performed subcellular fractionation to obtain the PSD of WT and Y876F cortical neurons treated with TTX for 48 h or left untreated (control). Consistent with our surface biotinylation, surface staining, and mEPSC recording results (Fig. 4), we noted increases in synaptic GluA1 and GluA2 in WT neurons but not in Y876F neurons after TTX treatment for 48 h (Fig. 6 *A*–*C*). We also observed enhanced levels of synaptic

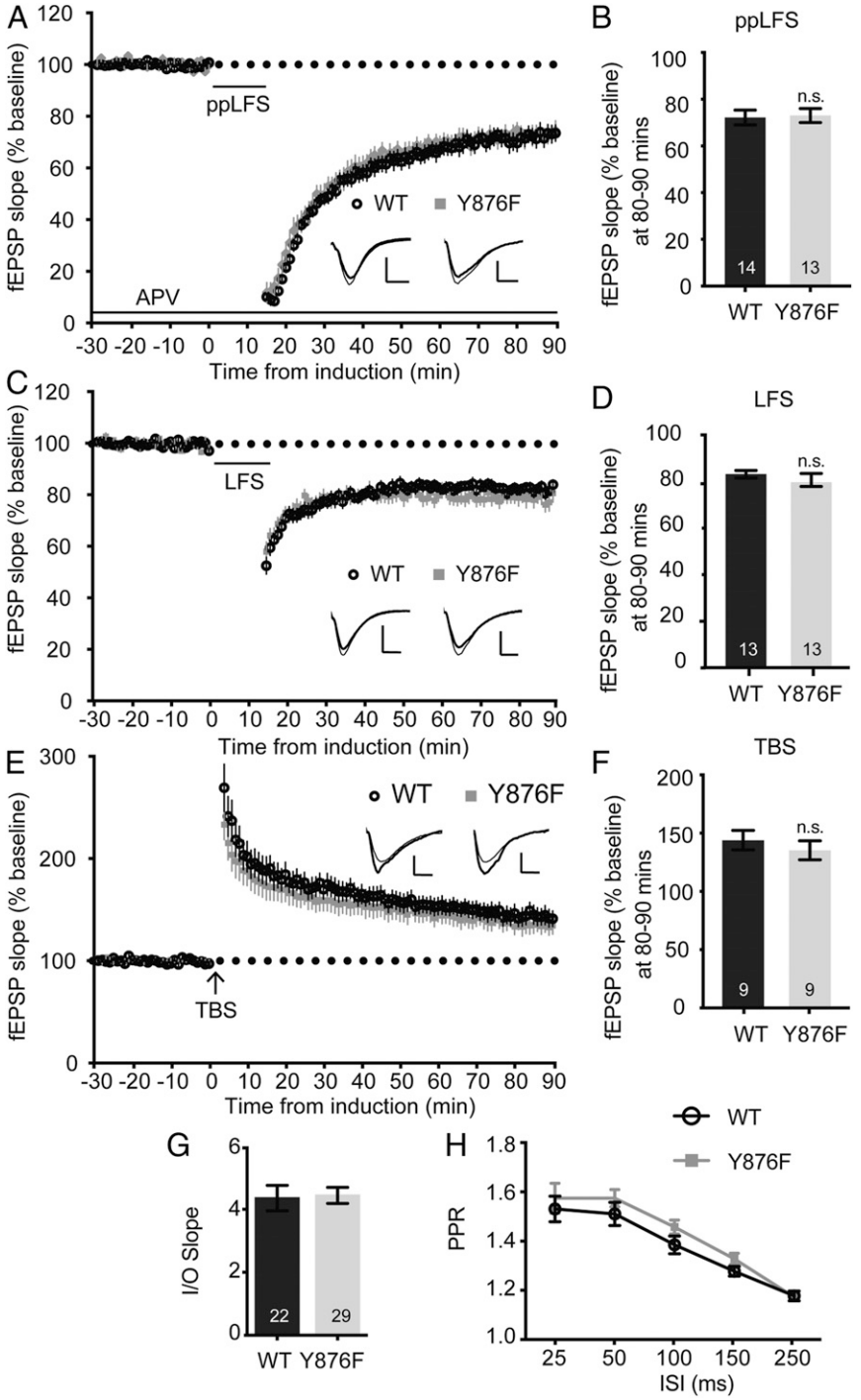

Fig. 2. GluA2 Y876F mice have normal Hebbian plasticity. Field recordings from Schaffer collateral-CA1 synapses from acute hippocampal slices from 2- to 5-mo-old male Y876F mice and WT littermates. Sample traces represent fEPSPs at one min before (thin) and 90 min after (thick) stimulation [Scale bars represent 0.5 mV (vertical) and 5 ms (horizontal)] (*A*) ppLFS-induced LTD in the presence of 50 μM D-APV. (*B*) Quantification of the magnitude of ppLFS-LTD 80 to 90 min after induction, normalized to baseline. $n = 13$–14, unpaired *t* test. Slices are from seven WT mice and five Y876F mice. (*C*) LFS-induced LTD. (*D*) Quantification of the magnitude of LFS-LTD 80 to 90 min after induction, normalized to baseline. $n = 13$, unpaired *t* test. Slices were from three WT mice and three Y876F mice. (*E*) TBS-induced LTP. (*F*) Quantification of the magnitude of TBS-LTP 80 to 90 min after induction, normalized to baseline. $n = 9$, unpaired *t* test. Slices were from five WT mice and six Y876F mice. (*G*) Slope of I/O relationships of fEPSPs. $n = 21$ to 29, unpaired *t* test. (*H*) PPRs with different interstimulus intervals (ISIs). $n =$ 15 to 24, two-way ANOVA.

GRIP1 (Fig. 6 *A* and *D*), a finding that agrees with previous studies (32, 33). In contrast, no increases in synaptic GRIP1 were observed in Y876F neurons (Fig. 6 *A*–*D*). Furthermore, we examined GRIP1 in the V1 PSD of WT and Y876F mice after enucleation, and found an increase in WT mice but not in Y876F mice (Fig. 6 *E* and *F*). These results indicate that GluA2 pY876 is necessary for synaptic GRIP1 increase during upscaling.

Phosphorylation of GluA2 Y876 Increases Binding of GRIP1 to GluA2. Since the synapses of Y876F mice do not accumulate GRIP1

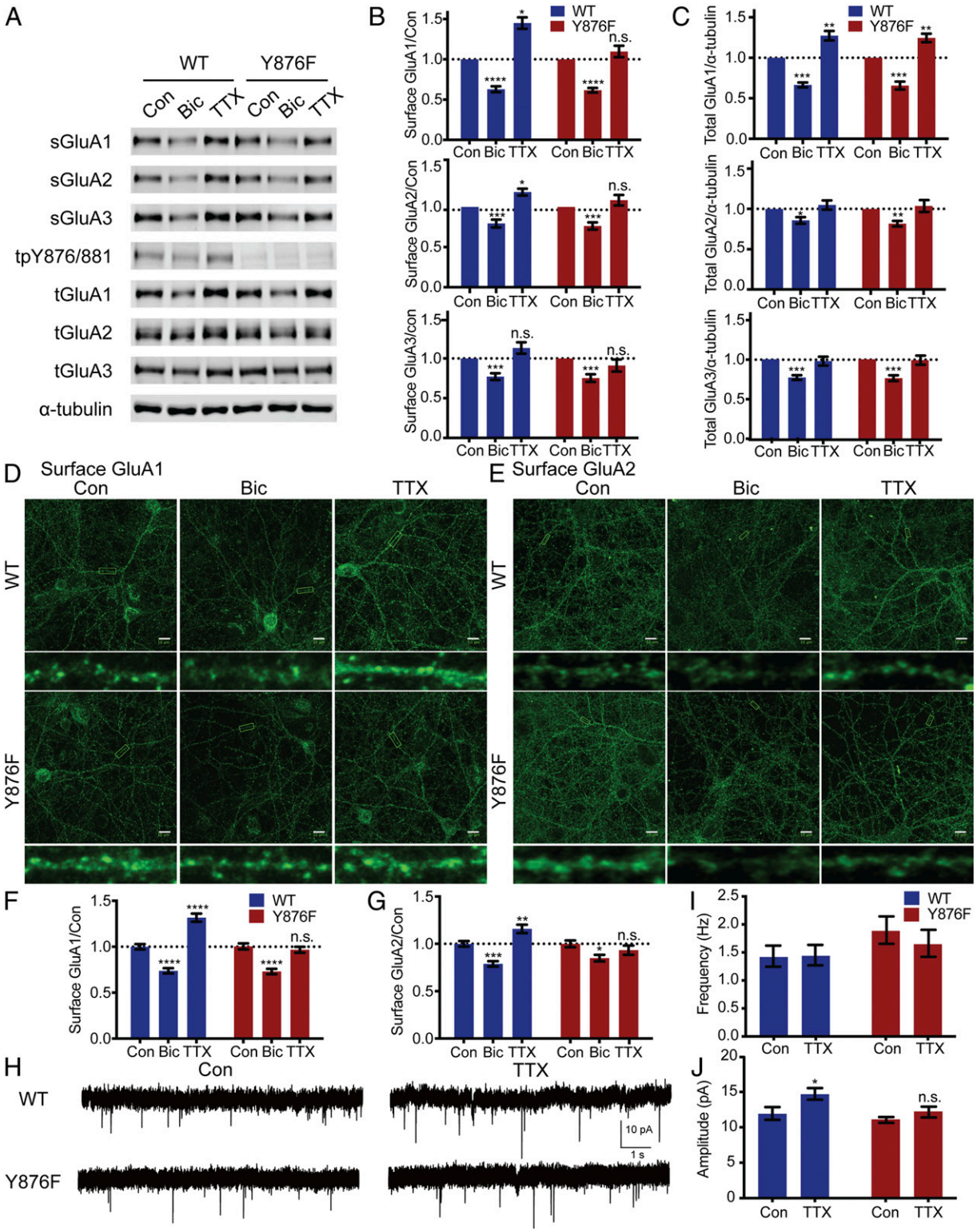

Fig. 3. TTX-induced upscaling is deficient in GluA2 Y876F cultured neurons. (*A*, *D*, *E*, and *H*) WT and Y876F mutant mouse cortical neurons at DIV11–13 were untreated (Con) or treated with 20 μM Bic or 1 μM TTX for 48 h followed by surface biotinylation and Western blot (*A*), surface staining (*D* and *E*), or whole-cell recording (*H*). (*A*) *s* refers to surface levels; *t* refers to total levels. (*B*) Quantification of cell surface levels of GluA1, GluA2, and GluA3 from (*A*) normalized to control. $n = 4$–8, one-sample *t* test. (*C*) Quantification of total levels of GluA1, GluA2, and GluA3 from (*A*) normalized to tubulin and control. n= 4–8, one-sample *t* test. (*D* and *E*) Surface GluA1 (*D*) and surface GluA2 (*E*) were labeled using an anti-N-terminal antibody under nonpermeabilized conditions. (Scale bar, 10 μm.) A representative dendrite from each neuron was magnified. (*F* and *G*) Surface levels of GluA1 (*F*) or GluA2 (*G*) were quantified from 10 to 12 dendritic segments each from 22 to 36 neurons, from 2 to 3 sets of staining experiments from *D* and *E*, normalized to control, two-way ANOVA. (*H*) Representative traces from mEPSC recordings. (*I* and *J*) Quantification of mEPSC frequency (*I*) or amplitude (*J*). $n = 13$–21, two-way ANOVA. $^*P < 0.05$, $^{**}P < 0.01$, $^{***}P < 0.001$, $^{****}P < 0.0001$.

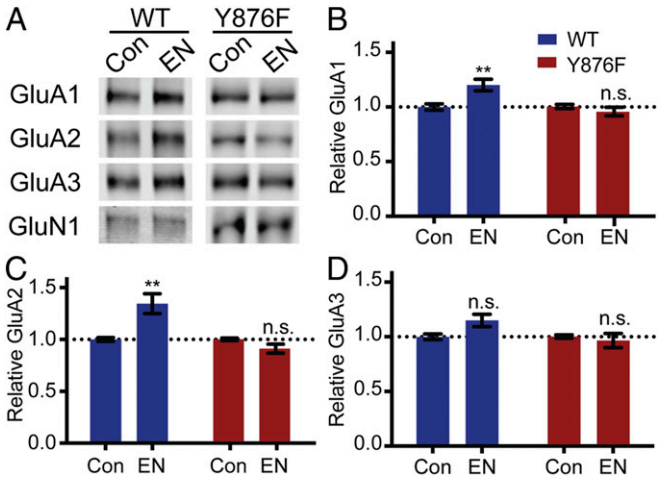

Fig. 4. GluA2 Y876F mice do not undergo visual-deprivation–induced in vivo upscaling. Male WT or Y876F mice at postnatal (P)63–121 underwent sham treatment (Con) or binocular enucleation (EN) to induce visual deprivation, and their primary visual cortex was harvested after two or seven d. (*A*) PSD of V1 was obtained through subcellular fractionation followed by Western blot. (*B–D*) Quantifications of (*A*) GluA1, GluA2, and GluA3 were normalized to GluN1 and control. $n = 11–12$, two-way ANOVA. $^{**}P < 0.01$.

during upscaling, these data suggest that phosphorylation of Y876 can regulate the binding of GRIP1 to GluA2. To test this possibility directly, we modulated phospho-Y876 levels and measured binding of GRIP1 to GluA2. First, we used WT and Y876F cultured cortical neurons and treated them with NV, which increases tyrosine phosphorylation, including phospho-Y876 (Fig. 7*B*), followed by coimmunoprecipitation (Co-IP) with an anti-GRIP1 antibody (Fig. 7*A*). When we immunoblotted for GluA2 and normalized it to the amount of immunoprecipitated GRIP1, we found increased GRIP1–GluA2 binding after NV treatment in cultures from WT but not from Y876F mice (Fig. 7*C*), indicating that an increase in phosphorylation of Y876 enhances GRIP1 binding to GluA2. In addition, we performed another Co-IP using an anti-GluA2 antibody and immunoblotted for GRIP1 (*SI Appendix*, Fig. S6*A*). Similar to the previous experiment, we observed an increase in GRIP1 binding to GluA2 with NV treatment in WT but not Y876F neurons (*SI Appendix*, Fig. S6*C*). As an alternate strategy, we performed a comparable experiment in HEK293 cells by overexpressing WT or Y876F GluA2, together with GRIP1-GFP and Fyn, a kinase that phosphorylates GluA2 Y876 (13). Then we performed Co-IPs using an anti-GFP antibody. The expression of Fyn with WT GluA2 not only increased phosphorylation of Y876 (Fig. 7*D*) but also enhanced GluA2 binding to GRIP1 (Fig. 7 *D* and *E*). Notably, this increase in binding to GRIP1 was not observed in Y876F GluA2 when Fyn was overexpressed (Fig. 7 *D* and *E*), indicating that phospho-Y876 directly affects GRIP1 binding to GluA2.

Discussion

This study examined the role of phospho-Y876 on the AMPAR GluA2 subunit from three angles: how it affects synapses at baseline, its necessity in Hebbian plasticity, and its role in homeostatic plasticity. We found that GluA2 Y876 phosphorylation is important for the synaptic localization of GluA2. Additionally, phospho-Y876 is not essential for LTP or LTD, but is required for synaptic upscaling. A bidirectional regulation of phospho-Y876 in synaptic scaling occurs, with GluA2 phospho-Y876 decreasing during downscaling and increasing during upscaling. The increased phospho-Y876 in upscaling causes more GRIP1 to bind to GluA2, which favors AMPAR trafficking to and/or

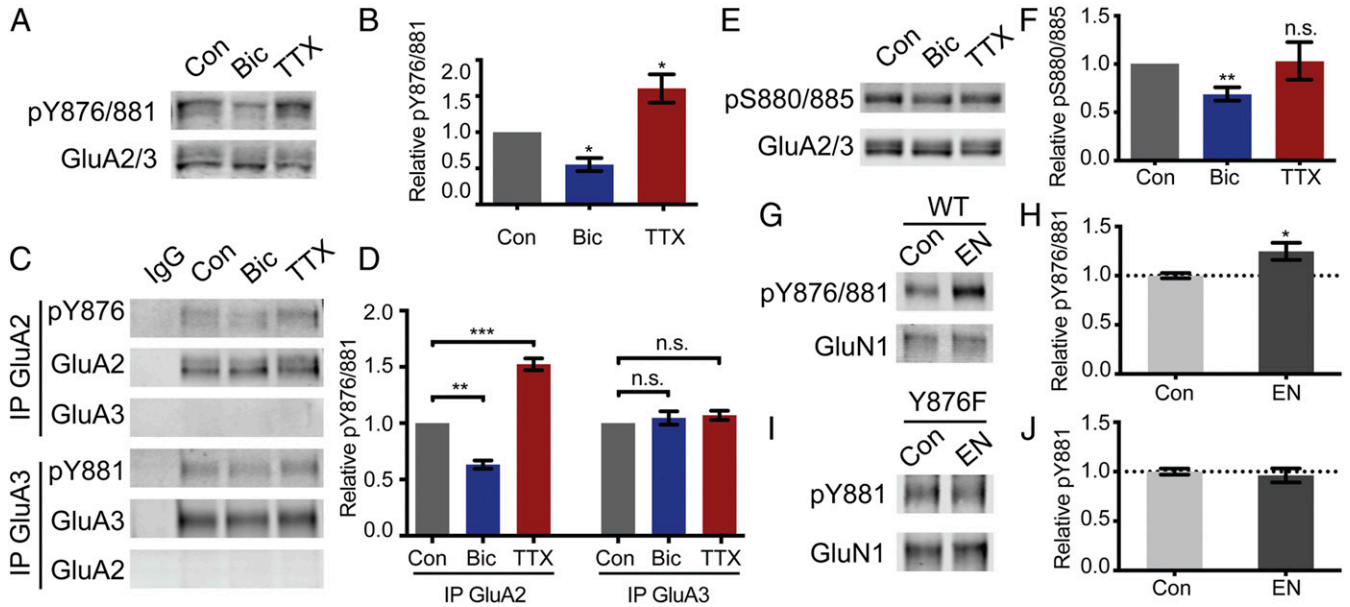

Fig. 5. Synaptic scaling bidirectionally regulates GluA2 phospho-Y876 but not GluA3 phospho-Y881. (*A*, *C*, and *E*) DIV11–13 rat cortical neurons were untreated (Con) or treated with 20 μM Bic or 1 μM TTX for 48 h, followed by a fully denaturing lysis and Western blot (*A* and *E*) or immunoprecipitation for GluA2 or GluA3 followed by Western blot (*C*). (*B*) Quantification of pY876/881 levels normalized to GluA2/3 and control from (*A*). $n = 3–5$, one-sample *t* test. (*D*) Quantification of pY876 or pY881 levels normalized to immunoprecipitated GluA2 or GluA3 and control, respectively, from (*C*). $n = 3–5$, one-sample *t* test. (*F*) Quantification of pS880/885 levels normalized to GluA2/3 and control from (*E*). $n = 6$, one-sample *t* test. (*G* and *I*) Male WT or Y876F mice at postnatal (P)63–121 underwent sham treatment (Con) or binocular EN to induce visual deprivation, and their primary visual cortex was harvested after two or seven d. PSD of V1 was obtained through subcellular fractionation followed by Western blot. (*H*) Quantification of (*G*) shows phosphorylation of GluA2 Y876 and GluA3 Y881 in WT mice normalized to GluN1 and control. $n = 11–12$, unpaired *t* test. (*J*) Quantification of (*I*) shows GluA3 Y881 phosphorylation of Y876F mice normalized to GluN1 and control, $n = 11–12$. Unpaired *t* test. $^{*}P < 0.05$, $^{**}P < 0.01$, $^{***}P < 0.001$.

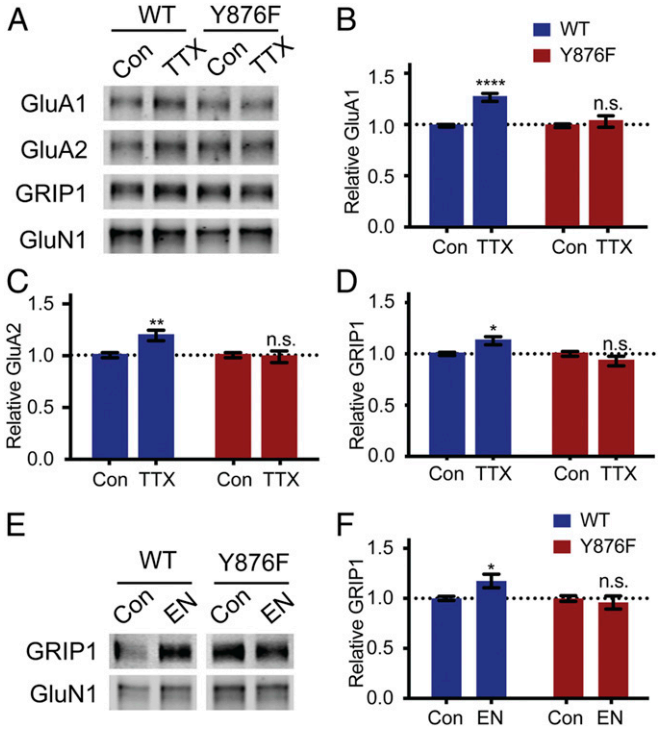

Fig. 6. GRIP1 does not increase in the synapses of GluA2 Y876F mice during upscaling. (*A*) WT and Y876F mouse cortical cultures were untreated (Con) or treated with TTX for 48 h. PSD preparation was conducted followed by Western blot. (*B* and *C*) Quantification of GluA1 (*B*), GluA2 (*C*), and GRIP1 (*D*) from (*A*) normalized to GluN1 and control. $n = 12$, two-way ANOVA. (*E*) WT and Y876F mice underwent sham treatment (Con) or binocular EN for two or seven d. PSD was obtained, followed by Western blot for GRIP1. (*F*) Quantification of *D*, normalized to GluN1 and control. $n = 10$–12, two-way ANOVA. $^{*}P < 0.05$, $^{**}P < 0.01$, $^{****}P < 0.0001$.

retention in synapses, a process that is critical for synaptic AMPAR increase in upscaling.

GluA2 Y876 and GluA3 Y881 Phosphorylation. Using immunoprecipitation and HEK293 cell experiments, we discovered that GluA3 is phosphorylated on Y881 by Src-family tyrosine kinases. In addition, we found that GluA3 S885 is phosphorylated by PKC and can also be detected by the GluA2 pS880 antibody. By comparing pY876/881 signals from WT and Y876F mice, we showed that, endogenously, the majority of the pY876/881 signal (~70%) is contributed by GluA2 phospho-Y876. Additionally, in the absence of GluA2 Y876 phosphorylation in adult Y876F mice, there were no compensations in GluA3 Y881 phosphorylation at basal levels. The study that first discovered GluA2 Y876 phosphorylation characterized its effects in cultured neurons using overexpression of GFP-GluA2 and found that surface and synaptic GluA2 decreased in Y876F mutants compared to WT at the basal state (13). Likewise, we observed that Y876F knock-in mice have decreased synaptic GluA2, with no change in total GluA2, indicating that phosphorylation of GluA2 Y876 plays an important role in trafficking to and/or maintaining GluA2 at synapses in basal states. While the other AMPAR subunits, GluA1 and GluA3, did not show a significant decrease in the synapse, we noted a trend toward a decrease in GluA3 (P value = 0.00828 before multiple t test correction using the Holmes-Sidak method, and P value = 0.117 after correction), indicating that the affected population most likely consists of GluA2/3 AMPARs.

GluA2 Y876 is close to GluA2 S880, the phosphorylation of which is known to increase GluA2 endocytosis. Using peptides, we verified that the pY876/881 antibody is not affected by the phosphorylation status of GluA2 S880. A previous study using in vitro kinase assays concluded that phosphorylation at Y876 inhibits phosphorylation of S880 by PKC (23). However, this result is confounded by the possibility that the phosphorylation status of Y876 itself could affect the binding affinity of the previous study of pS880 antibody to pS880. We used peptides to show that the ability of our pS880 antibody to detect pS880 is unaffected by phosphorylation status at the Y876 site. With this, we can reliably conclude that the ability of Src kinase to phosphorylate Y876/881 is not affected by phospho-S880/885, nor is protein kinase C's ability to phosphorylate S880/885 affected by the phosphorylation status of Y876/881. Additionally, we showed that phospho-S880/885 phosphorylation in Y876F knock-in mice is unchanged, indicating that the effect of Y876 on decreased synaptic GluA2 is not due to an increase in phospho-S880.

Despite a decrease in synaptic GluA2, we found no changes in the synaptic expression of scaffolding or trafficking proteins, including GRIP1 and PICK1. Hence it is likely that, in basal states, phospho-Y876 is important for tethering to preexisting trafficking or synaptic scaffold proteins, without affecting the trafficking machinery or the synaptic scaffold itself. At basal levels, it appears that localization of GRIP1 to the synapse is not dependent on the phosphorylation status of GluA2 Y876.

GluA2 Y876 Phosphorylation in Homeostatic Scaling. Changes in the phosphorylation of GluA1 S845 are necessary for both TTX-induced and visual-deprivation–induced upscaling (7, 8). However, studies have shown that GluA2 but not the GluA1 subunit is required for upscaling and that its cytoplasmic tail is indispensable in this process (34, 35). In agreement with a previous study (7), we observed a decrease in S880 phosphorylation during synaptic downscaling, with no change during upscaling. Bidirectional regulation of GluA2 tyrosine phosphorylation has been reported, with a decrease during downscaling and an increase during upscaling (24). However, they were unable to pinpoint the tyrosine site(s) on which the change occurred. It is possible that phosphorylation of one or two or all three sites change during synaptic scaling. We generated an antibody specific for pY876/881 and found bidirectional regulation of phospho-Y876/881 (Fig. 5 *A* and *B*). Since GluA2 Y876 and GluA3 Y881 are both phosphorylated by Src-family tyrosine kinase, and GluA2 and GluA3 C termini are homologous, we speculated that they would be regulated similarly and play redundant roles. However, it was interesting that, while GluA2 phospho-Y876 showed bidirectional regulation during synaptic scaling, levels of GluA3 phospho-Y881 remained unchanged. Furthermore, we found that phospho-Y876 is necessary for upscaling, as neither TTX treatment nor visual deprivation could induce upscaling in Y876F mice. More studies are needed to show how GluA3 Y881 phosphorylation is regulated, especially how it can be controlled independently of GluA2 Y876 phosphorylation.

Our phospho-Y876/881 antibody picks up both GluA2 phospho-Y876 and GluA3 phospho-Y881 signals. Since the amount of protein that we obtained from V1 PSD was very little (~20 ug), it was not enough for us to probe multiple proteins (including the GluA2/3 signal) and definitely not enough to perform IP (which would need ~500 ug protein). Hence, it would be hard for us to normalize the pY876/881 signal to GluA2, GluA3 (which would require IPs), or GluA2/3 (which would need more protein). Instead, we chose to normalize the pY876/881 signal to GluN1, as we know that GluN1 does not change with synaptic upscaling. When we normalized the pY876/881 signal to GluA2, we saw a trend toward an increase, although the increase was not significant (*SI Appendix*, Fig. S7). This suggests that GluA2 phosphorylation at Y876 may be enhanced by binocular enucleation. We know that pY881 does not change (Fig. 5 *G*–*J*) but GluA2 increases in the synapse (Fig. 4*C*). If pY876/881 is normalized to GluA2, because pY881 is not increasing even if pY876 is increasing at the same

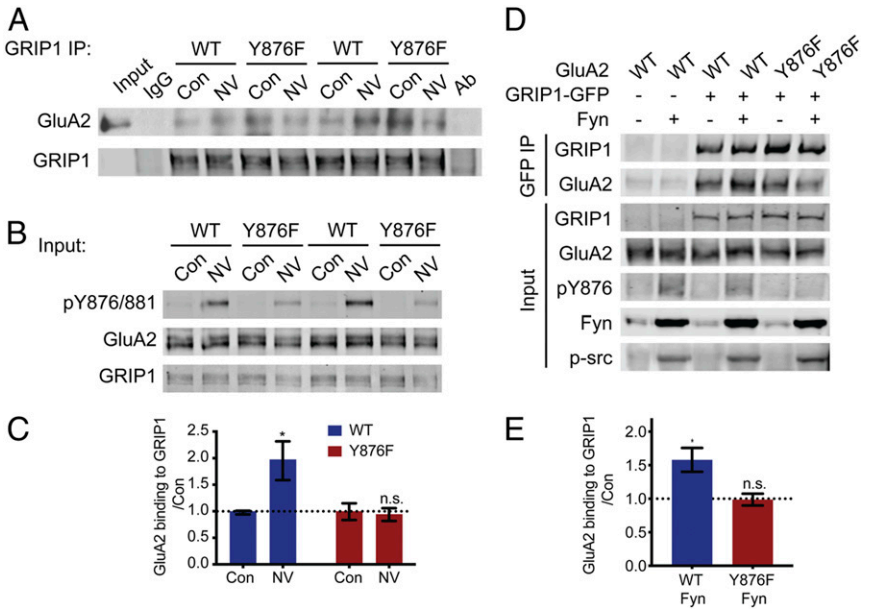

Fig. 7. Phosphorylation of GluA2 Y876 increased GRIP1 binding to GluA2. (*A* and *B*) WT and Y876F mouse cortical cultures were untreated (Con) or treated with 1 μM NV overnight, followed by Western blot (*B*) or coimmunoprecipitation with GRIP1 antibody and Western blot (*A*). (*A*) Coimmunoprecipitation control includes rabbit immunoglobulin control (IgG) and antibody-only control (Ab). (*C*) Quantification of (*A*) with GluA2 normalized to GRIP1 and control. $n = 4$, two-way ANOVA. (*D*) HEK293 cells were transfected with WT or Y876F GluA2, GRIP1-GFP, and Fyn for two d, followed by coimmunoprecipitation for GluA2 using a green fluorescent protein (GFP) antibody. (*E*) Quantification of (*D*), immunoprecipitated GluA2 was normalized to GRIP1 and control. $n = 4$, one-sample *t* test. $^*P < 0.05$.

proportion with GluA2, the normalized signal of pY876/881 to GluA2 actually decreases. However, we see a trend toward an increase in the normalized signal, indicating that pY876 increases more than GluA2 following visual deprivation.

Phosphorylation levels are regulated by the opposing activities of phosphatases and kinases. Synaptic scaling changes the expression and activity of striatal-enriched protein tyrosine phosphatase 61 kDa (STEP61), a tyrosine phosphatase that is enriched in the brain (24). Upscaling increases STEP61 activity, while downscaling decreases its activity (24). Infusion of transactivator of transcription (TAT)-STEP, a membrane-permeable version of STEP, during TTX treatment decreases GluA2 3Y phosphorylation and also blocks the increase in mEPSC amplitude (24). These results suggest that the increase in tyrosine phosphorylation of GluA2 during TTX treatment is due to a decrease in STEP61 levels and/or activity, while the decrease with Bic treatment occurs from an increase in STEP61 levels and/or activity. Given these results, we believe that STEP61 is a likely candidate to dephosphorylate GluA2 Y876 and play a role in regulating phospho-Y876 during synaptic scaling. GluA2 Y876 is known to be phosphorylated by Src-family tyrosine kinases (13, 14). Among these kinases, Src, Fyn, Lyn, and Yes show high expression in the central nervous system (36). Changes in Src-family kinase activity may also account for the regulation of phospho-Y876. It is possible that the coordination of phosphatase and kinase activities accounts for the changes in GluA2 Y876 phosphorylation in synaptic scaling.

One study using organotypic hippocampal slices found that a specific residue, A843 GluA2, in the membrane-proximal region of the GluA2 cytoplasmic tail is necessary for upscaling (34). However, it is known that GRIP1, which binds to the PDZ ligand (amino acids 880 to 883) on GluA2, is necessary for upscaling in dissociated cortical cultures (32, 33). Hence, it is more likely in our cortical culture system that residues on or close by the PDZ ligand can affect GRIP1 binding and be crucial for upscaling. Another study observed that upscaling is normal following overexpression of GluA2 Y876F in GluA2 knock-down cortical neurons but is eliminated with GluA2 Y876E (33). We believe that these discrepancies are also due to a difference in models, as this study used RNA knockdown and overexpression replacement strategies that might have had off-target effects, while we used a knock-in mouse with all GluA2 subunits phospho-deficient at Y876 at endogenous levels.

Tyrosine Phosphorylation in Hebbian Plasticity. Many studies utilizing the GluA2 3Y peptide in LTD experiments have observed the same phenomenon: a significant reduction in LTD. These results suggest that the three tyrosine sites are critical for activity-regulated GluA2 endocytosis. While in some studies it is unclear whether the tyrosine sites themselves are necessary, other studies have used a control with the tyrosines mutated to alanines (3A) and have found that LTD appears normal with the control. These studies show that LFS-LTD (12, 18–20) and ppLFS-LTD (19) are abolished with the GluA2 3Y peptide. This effect has also been replicated in vivo (16). Presumably, there are proteins that bind to endogenous GluA2 3Y, likely depending on their phosphorylation status, leading to AMPAR endocytosis; and the GluA2 3Y peptide can competitively bind to those proteins to prevent endocytosis. However, studies seem to differ about the contribution of GluA2 tyrosine phosphorylation in different forms of LTD. LFS-LTD increases GluA2 tyrosine phosphorylation (12) while mGluR-LTD decreases GluA2 tyrosine phosphorylation (21, 22). Among the three tyrosine sites, only GluA2 Y876 has been validated to be phosphorylated (13, 14, 23). One study found that dephosphorylation of GluA2 Y876 occurs during mGluR-LTD, allowing BRAG2 to bind to GluA2, which activates Arf-6, resulting in GluA2 internalization (14). The same study also shows that, while the GluA3Y peptide can block mGluR-LTD, mutation of Y876 to V876 eliminates that blockage (14), which points to GluA2 Y876 as being critical for mGluR-LTD. With this plethora of studies on GluA2 tyrosine phosphorylation, there is much interest in the field about whether the changes in GluA2 tyrosine phosphorylation, particularly GluA2 Y876, are necessary for LTD.

mGluR-LTD and NMDAR-LTD are normal in GluA2 Y876F knock-in mice, proving that GluA2 phospho-Y876 is not necessary in LTD. It is possible that, during LTD, compensation with

GluA3 phopspho-Y881 occurs in GluA2 Y876F mice. The effect of the GluA2 3Y peptide on LTD in previous studies may also be due to its interference with GluA3 or the other two GluA2 tyrosine sites. We also observed that GluA2 Y876F knock-in mice have normal NMDAR-LTP. This result is perhaps not unexpected, since normal hippocampal LTP has been observed with treatment of the GluA2 3Y peptide (18).

Synaptic scaling shares overlapping mechanisms with Hebbian plasticity, such as the increase in GluA1 phospho-S845 by PKA during upscaling and LTP (5). Moreover, inducing upscaling or downscaling in neurons can respectively occlude or block LTP(7), indicating a convergence in pathways. Here, we show a mechanism that makes synaptic scaling distinct from Hebbian plasticity—while GluA2 phospho-Y876 is necessary for synaptic upscaling, it is not required for LTP or LTD. While changes in GluA2 phospho-Y876 occur during mGluR-LTD (14), we show that this change is not required for this process. On the other hand, the changes in GluA2 phospho-Y876 during synaptic scaling are critical for upscaling.

In conclusion, we uncover the molecular mechanisms behind the necessity of GluA2 in homeostatic scaling. Moreover, we show that the requirement of GluA2 phospho-Y876 is one of the mechanisms that is unique to synaptic scaling and not Hebbian plasticity.

Materials and Methods

Animals. All procedures related to animal husbandry and treatment were in accordance with Johns Hopkins University Animal Care and Use Committee guidelines. Sprague-Dawley rats (Harlan Laboratories) were used for cortical cultures at embryonic day 18 as described below. All animals were housed in a standard 12-h light/12-h dark cycle.

Binocular Enucleation. Male mice were anesthetized for a short period with isoflurane vapor and both eyes were surgically removed (37). Antibiotic ointment was applied and carprofen was administrated immediately after the enucleation. Control mice were given time-matched anesthesia and received antibiotic ointment treatment and carprofen administration. After the procedure, mice were returned to their home cage and monitored daily to make sure there was no bleeding or infection.

Lysis Buffers. All lysis buffers contained 200 nM okadaic acid, 2.5 mM Na_3VO_4, protease inhibitor mixture (Roche), and PhosSTOP phosphatase inhibitor (Roche).

Pellet 2 (P2) and PSD Preparation. Samples were kept on ice throughout the experiment, and centrifugations were conducted at 4 °C. P2 and PSD were prepared as in Chiu et al. (38). The final PSD pellet was resuspended in lysis buffer [phosphate-buffered saline (PBS)] with 50 mM sodium flouride, 5 mM sodium pyrophosphate, 1 mM ethylenediaminetetraacetic acid (EDTA), 1 mM ethylene glycol-bis(β-aminoethyl ether)-*N*,*N*,*N*′,*N*′-tetraacetic acid (EGTA) 1% Nonidet P-40, 0.5% sodium deoxycholate, 0.1% sodium dodecyl sulfate, sonicated, and followed by protein quantification and Western blot.

Immunocytochemistry. For surface AMPA receptor labeling, neurons were fixed for 4 min in PBS containing 4% paraformaldehyde (PFA)/4% sucrose and rinsed with PBS. Blocking was done in 10% bovine serum albumin (BSA) in PBS for 30 min before incubation with N-terminus mouse anti-GluA1 or mouse anti-GluA2 antibodies in PBS with 1% BSA for 3 h at room temperature. Coverslips were washed with PBS before the neurons were permeabilized with 0.25% Triton X-100 (Sigma-Aldrich) for 15 min followed by blocking as before. After rinsing with PBS, coverslips were incubated with Alexa Fluor 568-conjugated goat antimouse secondary antibodies (Molecular Probe) in PBS containing 1% BSA for 1h. After final washes with PBS, coverslips were mounted onto glass slides using Fluoromount-G (Southern Biotech). Images were obtained using an 880 laser scanning confocal microscope (Zeiss). Anti-GluA1 (4.9D, made in-house) and anti-GluA2 (15F1) antibodies were used for surface staining.

Image Analysis. All image analysis was done using ImageJ software (National Institutes of Health). For measurement of surface AMPAR expression, areas of nonprimary dendrites with clear surface GluA1 or GluA2 staining were manually traced and the mean fluorescent intensity per pixel of dendrite was recorded. The average intensity of 10 to 15 regions of dendrite per image was measured and used for analysis. For each image, a region devoid of dendrites was measured and used for background subtraction. For each condition shown, 20 to 30 images were used

Extracellular Field Recordings. One Y876F WT or knock-in male mice (2- to 5-mo old) was recorded each day in an interleaved, randomized manner. Field recording experiments were conducted as in Chiu et al. (38). All plasticity experiments were presented as responses normalized to the average of the 30-min baseline. Averages from 80 to 90 min were used for calculating the magnitude of plasticity and for statistical tests. mGluR-LTD was performed in the presence of APV and induced by paired-pulse LFS with 50-ms interpulse intervals of 900 pulses at 1 Hz.

Intracellular Whole-Cell Recordings. Electrical signals were acquired at 10 kHz with a Multiclamp 700B amplifier using pClamp10 software (Molecular Devices). Cells were held at −70 mV, and mEPSC measurements were collected for 7 to 10 min.

Quantification and Statistical Analysis. All data were presented as mean, with error bars indicating ± SEM (SE of the mean). All statistical details and statistical significance, calculated using the unpaired *t* test, one-sample *t* test, or two-way ANOVA, are indicated in the figure legends. Bonferroni post hoc tests were used following two-way ANOVA. $*P < 0.05$, $**P < 0.01$, $***P < 0.001$, $****P < 0.0001$; n.s., no statistical significance.

ACKNOWLEDGMENTS. We thank Dr. Eric Gouaux for the N-terminal GluA2 antibody and all members of the R.L.H. lab for helpful discussion and critical reading of the manuscript, especially Graham H. Diering and Sarah Richardson for experimental support. This work was supported by the NIH (NINDS R01NS036715 and NIA P50 AG005146).

1. R. C. Malenka, M. F. Bear, LTP and LTD: An embarrassment of riches. *Neuron* **44**, 5–21 (2004).
2. G. G. Turrigiano, K. R. Leslie, N. S. Desai, L. C. Rutherford, S. B. Nelson, Activity-dependent scaling of quantal amplitude in neocortical neurons. *Nature* **391**, 892–896 (1998).
3. G. G. Turrigiano, The self-tuning neuron: Synaptic scaling of excitatory synapses. *Cell* **135**, 422–435 (2008).
4. R. J. O'Brien *et al*., Activity-dependent modulation of synaptic AMPA receptor accumulation. *Neuron* **21**, 1067–1078 (1998).
5. G. H. Diering, R. L. Huganir, The AMPA receptor code of synaptic plasticity. *Neuron* **100**, 314–329 (2018).
6. J. D. Shepherd, R. L. Huganir, The cell biology of synaptic plasticity: AMPA receptor trafficking. *Annu. Rev. Cell Dev. Biol.* **23**, 613–643 (2007).
7. G. H. Diering, A. S. Gustina, R. L. Huganir, PKA-GluA1 coupling via AKAP5 controls AMPA receptor phosphorylation and cell-surface targeting during bidirectional homeostatic plasticity. *Neuron* **84**, 790–805 (2014).
8. A. Goel *et al*., Phosphorylation of AMPA receptors is required for sensory deprivation-induced homeostatic synaptic plasticity. *PLoS One* **6**, e18264 (2011).
9. J. P. Steinberg *et al*., Targeted in vivo mutations of the AMPA receptor subunit GluR2 and its interacting protein PICK1 eliminate cerebellar long-term depression. *Neuron* **49**, 845–860 (2006).
10. H. J. Chung, J. Xia, R. H. Scannevin, X. Zhang, R. L. Huganir, Phosphorylation of the AMPA receptor subunit GluR2 differentially regulates its interaction with PDZ domain-containing proteins. *J. Neurosci.* **20**, 7258–7267 (2000).
11. K. J. Seidenman, J. P. Steinberg, R. Huganir, R. Malinow, Glutamate receptor subunit 2 Serine 880 phosphorylation modulates synaptic transmission and mediates plasticity in CA1 pyramidal cells. *J. Neurosci.* **23**, 9220–9228 (2003).
12. G. Ahmadian *et al*., Tyrosine phosphorylation of GluR2 is required for insulin-stimulated AMPA receptor endocytosis and LTD. *EMBO J.* **23**, 1040–1050 (2004).
13. T. Hayashi, R. L. Huganir, Tyrosine phosphorylation and regulation of the AMPA receptor by SRC family tyrosine kinases. *J. Neurosci.* **24**, 6152–6160 (2004).
14. R. Scholz *et al*., AMPA receptor signaling through BRAG2 and Arf6 critical for long-term synaptic depression. *Neuron* **66**, 768–780 (2010).
15. A. Awasthi *et al*., Synaptotagmin-3 drives AMPA receptor endocytosis, depression of synapse strength, and forgetting. *Science* **363**, eaav1483 (2019).
16. C. J. Fox, K. Russell, A. K. Titterness, Y. T. Wang, B. R. Christie, Tyrosine phosphorylation of the GluR2 subunit is required for long-term depression of synaptic efficacy in young animals in vivo. *Hippocampus* **17**, 600–605 (2007).
17. Y. Ge *et al*., Hippocampal long-term depression is required for the consolidation of spatial memory. *Proc. Natl. Acad. Sci. U.S.A.* **107**, 16697–16702 (2010).
18. K. Brebner *et al*., Nucleus accumbens long-term depression and the expression of behavioral sensitization. *Science* **310**, 1340–1343 (2005).
19. R. L. Clem, R. L. Huganir, Norepinephrine enhances a discrete form of long-term depression during fear memory storage. *J. Neurosci.* **33**, 11825–11832 (2013).
20. S. Y. Yu, D. C. Wu, L. Liu, Y. Ge, Y. T. Wang, Role of AMPA receptor trafficking in NMDA receptor-dependent synaptic plasticity in the rat lateral amygdala. *J. Neurochem.* **106**, 889–899 (2008).

21. P. R. Moult *et al*., Tyrosine phosphatases regulate AMPA receptor trafficking during metabotropic glutamate receptor-mediated long-term depression. *J. Neurosci.* **26**, 2544–2554 (2006).
22. C. M. Gladding *et al*., Tyrosine dephosphorylation regulates AMPAR internalisation in mGluR-LTD. *Mol. Cell. Neurosci.* **40**, 267–279 (2009).
23. K. Kohda *et al*., The δ2 glutamate receptor gates long-term depression by coordinating interactions between two AMPA receptor phosphorylation sites. *Proc. Natl. Acad. Sci. U.S.A.* **110**, E948–E957 (2013).
24. S.-S. Jang *et al*., Regulation of STEP61 and tyrosine-phosphorylation of NMDA and AMPA receptors during homeostatic synaptic plasticity. *Mol. Brain* **8**, 55 (2015).
25. C. C. Huang, K. S. Hsu, Sustained activation of metabotropic glutamate receptor 5 and protein tyrosine phosphatases mediate the expression of (S)-3,5-dihydroxyphenylglycine-induced long-term depression in the hippocampal CA1 region. *J. Neurochem.* **96**, 179–194 (2006).
26. N. S. Desai, R. H. Cudmore, S. B. Nelson, G. G. Turrigiano, Critical periods for experience-dependent synaptic scaling in visual cortex. *Nat. Neurosci.* **5**, 783–789 (2002).
27. A. Goel, H.-K. Lee, Persistence of experience-induced homeostatic synaptic plasticity through adulthood in superficial layers of mouse visual cortex. *J. Neurosci.* **27**, 6692–6700 (2007).
28. A. Goel *et al*., Cross-modal regulation of synaptic AMPA receptors in primary sensory cortices by visual experience. *Nat. Neurosci.* **9**, 1001–1003 (2006).
29. K. He, E. Petrus, N. Gammon, H.-K. Lee, Distinct sensory requirements for unimodal and cross-modal homeostatic synaptic plasticity. *J. Neurosci.* **32**, 8469–8474 (2012).
30. V. Anggono, R. L. Huganir, Regulation of AMPA receptor trafficking and synaptic plasticity. *Curr. Opin. Neurobiol.* **22**, 461–469 (2012).
31. L. Mao, K. Takamiya, G. Thomas, D.-T. Lin, R. L. Huganir, GRIP1 and 2 regulate activity-dependent AMPA receptor recycling via exocyst complex interactions. *Proc. Natl. Acad. Sci. U.S.A.* **107**, 19038–19043 (2010).
32. H. L. Tan, B. N. Queenan, R. L. Huganir, GRIP1 is required for homeostatic regulation of AMPAR trafficking. *Proc. Natl. Acad. Sci. U.S.A.* **112**, 10026–10031 (2015).
33. M. A. Gainey, V. Tatavarty, M. Nahmani, H. Lin, G. G. Turrigiano, Activity-dependent synaptic GRIP1 accumulation drives synaptic scaling up in response to action potential blockade. *Proc. Natl. Acad. Sci. U.S.A.* **112**, E3590–E3599 (2015).
34. S. G. Ancona Esselmann, J. Díaz-Alonso, J. M. Levy, M. A. Bemben, R. A. Nicoll, Synaptic homeostasis requires the membrane-proximal carboxy tail of GluA2. *Proc. Natl. Acad. Sci. U.S.A.* **114**, 13266–13271 (2017).
35. M. A. Gainey, J. R. Hurvitz-Wolff, M. E. Lambo, G. G. Turrigiano, Synaptic scaling requires the GluR2 subunit of the AMPA receptor. *J. Neurosci.* **29**, 6479–6489 (2009).
36. T. Hayashi, H. Umemori, M. Mishina, T. Yamamoto, The AMPA receptor interacts with and signals through the protein tyrosine kinase Lyn. *Nature* **397**, 72–76 (1999).
37. J. Aerts, J. Nys, L. Arckens, A highly reproducible and straightforward method to perform in vivo ocular enucleation in the mouse after eye opening. *J. Vis. Exp.* **6**, e51936 (2014).
38. S.-L. L. Chiu *et al*., GRASP1 regulates synaptic plasticity and learning through endosomal recycling of AMPA receptors. *Neuron* **93**, 1405–1419.e8 (2017).